Intrinsic diffusion length of excitons in long single-walled carbon nanotubes from photoluminescence spectra

Jianping Xie,* Takumi Inaba, Ryohei Sugiyama, and Yoshikazu Homma†
Department of Physics, Tokyo University of Science, Shinjuku, Tokyo 162-8601, Japan
(Received 17 October 2011; revised manuscript received 29 December 2011; published 27 February 2012)

Evaluation of intrinsic diffusion length of excitons in a long single-walled carbon nanotube (SWNT) is reported by analyzing the tube-length dependence of photoluminescence (PL) emission intensity. The PL emission intensities depending on the tube length are all obtained from one individual long SWNT suspended on a groove-patterned substrate. The exciton dynamics is described by a one-dimensional diffusion equation. The diffusion length in the clean and pristine long SWNTs is found to be constant, about 200 nm at a lower laser power regime, indicating an intrinsic diffusion behavior. The threshold laser power that is consistent with the onset of exciton-exciton annihilation is about 10^{21} photons/(cm^2 s) for air-suspended SWNTs.

DOI: 10.1103/PhysRevB.85.085434 PACS number(s): 78.67.Ch, 71.35.−y, 78.55.−m

I. INTRODUCTION

Optical processes in single-walled carbon nanotubes (SWNTs) are dominated by the dynamics of the strongly correlated electron-hole pairs, i.e., excitons, which are confined in one dimension (1D) by Coulomb interaction with a large binding energy on the order of several hundred meV.[1,2] Excitons are diffusive in nature in SWNTs,[3] and exciton mobility is one of the fundamental properties for understanding the optical responses of SWNTs. In a diffusion model, exciton motion is characterized by diffusion length (L). All diffusing excitons move in a way proportional to $\sqrt{D\tau}$, independent of dimensionality. Here, D and τ are the diffusion coefficient and lifetime, respectively.

Up to now, many experimental studies have been carried out to investigate the exciton diffusion length in semiconducting SWNTs but leaving large scattering values. It differs by several orders of magnitude, ranging from 10^0 to 10^2 nm.[3–8] Most of those measurements were performed on ensemble samples which were surfactant- or DNA-wrapped, representing average results and preventing a detailed spectral analysis. The existence of tube to tube variations, such as the inhomogeneous linewidth or variation of photoluminescence (PL) intensity and emission energy could also reduce the reliability of the data. Discrepancy among the experimental results above has not yet been clarified. On the other hand, it is expected that the transport properties of excitons are extremely sensitive to their surroundings,[6] and exciton motion is strongly affected by trapping states and laser power.[7,8] Therefore, fabrications of well-separated SWNTs with a high quality are essential for investigating their intrinsic electronic and photonic properties.

Furthermore, for understanding the basic physics and future applications, it is believed that the intrinsic diffusion length of the excitons in SWNTs is of essential importance. For example, the intrinsic L relates to single-exciton SWNT device applications since the design of device size is determined by L for avoidance of the exciton-exciton annihilation (EEA) effect. Excitons move a significant distance before recombination in SWNTs transporting energy from one point to another. This may also open up a possibility for energy transfer or collection.

In this paper, we study the intrinsic diffusion length of excitons in long SWNTs suspended on groove-patterned substrates by PL spectra. We designed a SWNT-sample structure. Tube-length dependence of SWNT PL intensities was used to evaluate the diffusion length, and more importantly, the dependence of PL intensity on tube length l was obtained from the same long SWNT suspended on the groove-patterned substrate. The result of experiment shows that the exciton diffusion length in freely suspended SWNTs can be as large as 200 nm. The laser power independence of diffusion length in a lower power regime shows an intrinsic diffusion nature of excitons, which has not been clearly recognized in the previous papers.[3–8] Additionally, the onset laser power where the EEA begins to significantly affect the diffusion length is also analyzed.

II. EXPERIMENT

SWNTs were prepared on a well-designed groove-patterned quartz crystal substrate by a gas flow guided method in alcohol chemical vapor deposition.[9] The groove width on the substrates varied from 200 to 800 nm periodically with a depth of about 300 nm fabricated by the lithography method [see Fig. 1(a)]. Fe catalyst for SWNT growth was deposited with a vacuum evaporator. The catalyst area and patterned substrate were separated. Long SWNTs grew on the catalyst-deposited area and extended to the receiving patterned substrate by gas flow. Long SWNTs were synthesized perpendicularly to the direction of the grooves.

A scanning electron microscopy (SEM) image of our typical individual long-SWNT sample is shown in Fig. 1(a). In SEM images, the suspended and unsuspended segments of SWNTs can be easily identified by the bright contrast due to the electron beam-induced current phenomenon between the silica substrate and SWNTs.[10] Figure 1(b) shows the atomic force microscopy (AFM) image of a long SWNT suspended on two typical grooves. Both of the SEM and AFM images demonstrate the successful synthesis of nicely suspended SWNTs.

For the PL measurements, a Ti:sapphire laser (690–870 nm, Coherent) was used as the excitation laser which was focused by an objective lens (50×) to a spot size of approximately 1.6 μm in diameter. The polarization of the laser is set to be parallel to the z axis of the SWNTs. PL spectra were collected by a spectrometer (SpectraPro 2300i, Princeton Instruments)

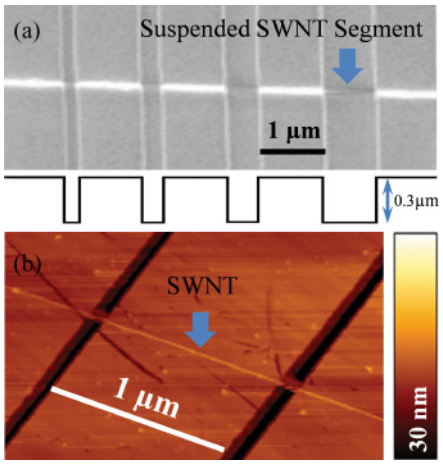

FIG. 1. (Color online) (a) Top: An SEM image of a long SWNT suspended on groove-patterned quartz substrate with diverse groove widths. Bottom: Schematic cross section of the groove-patterned substrate. (b) A typical AFM image of a long SWNT freely suspended on two grooves.

and an InGaAs multi-array detector (1024 channels, Princeton Instruments), which was cooled by liquid nitrogen to −100 °C. The emission spectra were measured from 900 to 1600 nm in atmosphere at room temperature. Semiconducting SWNTs that had intense and sharp emission peaks with narrow full width at half maximum (FWHM), which were thought to be high-quality SWNTs with few defects, were carefully chosen in advance for the experiments.

SWNTs are nonluminescent on silica (unsuspended segments) due to the significant substrate-induced nonradiative decay of excitons.[11] The nonluminescent features of the unsuspended carbon nanotube segments in our sample were checked by PL xy scanning. Therefore, we here assumed a perfect quencher at $|z| \geqslant l/2$ (set the origin to be at the center of the grooves), and only the suspended segments contributed to SWNT PL. Because the results were more or less the same among several high-quality SWNTs measured, the results obtained from a SWNT are shown in the following.

III. RESULTS AND DISCUSSION

A. Results of PL measurement

The studied SWNT was first identified by a PL excitation map where the first and second subband transition energies could be determined.[12] A typical PL excitation map performed on a suspended segment, 800 nm long, is shown in Fig. 2(a). The resonant excitation and emission wavelengths were found at 830 nm and 1483 nm, respectively. Those are consistent with the chirality of (11, 7) with a diameter of 1.2 nm, considering the wavelength shift for air-suspended SWNTs.[12–14] However, we should note that small blueshifts of excitation and emission wavelengths were observed for shorter nanotube segments. The origin of the small blueshifts will be discussed later.

Subsequently, the dependence of PL intensities on tube length was obtained by resonantly exciting ($\lambda = 830$ nm) the different suspended segments from the same SWNT. Figure 2(b) shows the measured emission spectra at excitation

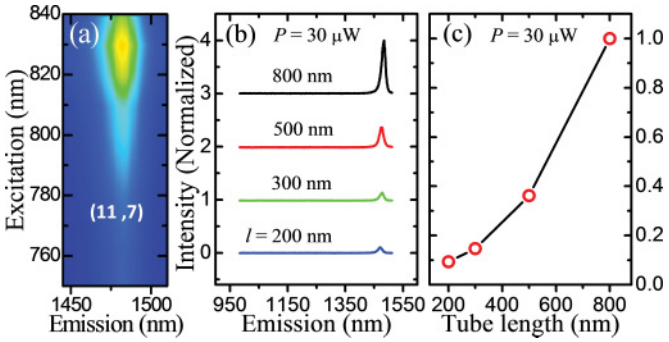

FIG. 2. (Color online) (a) Photoluminescence excitation map of the studied freely suspended SWNT. The SWNT can be assigned to a chirality of (11, 7) with a diameter of 1.2 nm. (b) Emission spectra (normalized intensity) from diverse tube segments at excitation power of 30 μW. The spectra are shifted for clarity. (c) Photoluminescence intensity as a function of tube length corresponding to (b). The solid line is a guide to the eye.

laser power (P) of 30 μW for tube length varying from 200 to 800 nm. The PL intensities increase with tube length as shown in Fig. 2(c). In addition, the time traces of PL intensity were also performed to check the PL stability (data not shown here). The stability of the PL intensity for a fixed suspended segment verified that the nanotube studied here showed no spectral shifts, broadening, or change in the emission intensity (PL blinking) during the experimental duration.

Because of the larger laser spot size, with increasing of l, we did not observe any saturation of PL intensity with $l \leqslant 800$ nm. However, it is expected that PL intensity will finally saturate when l is larger than the laser spot size. In that case, most of the excitons recombine before they diffuse to the unsuspended segments, and after that, l does not play a role for the PL intensity.[7]

Additionally, for each fixed suspended tube segment of the SWNT, we collected a series of PL spectra as a function of laser power. Figure 3(a) shows three typical emission spectra with excitation laser power of 7.7, 15, and 30 μW for $l = 800$ nm. As depicted in Fig. 3(b), it is found that PL intensity raises as excitation laser power increases. It scales linearly with P in the lower power regime. However, it deviates from the linearity at a higher power. The inset is the log-log plot of the main graph of Fig. 3(b). The solid red straight lines are the linear fittings in the lower power regime. The black arrows in both the inset and main graphs indicate the onset power where the nonlinearity occurs. The onset power can be read approximately 30 μW corresponding to a photon fluence of about 10^{21} photons/(cm^2 s). The nonlinear behavior is attributed to the EEA effect.[15–17] Generally, a larger laser power induces a larger number of excitons; correspondingly, there is a higher probability for EEA. If the EEA process is sufficiently efficient, it will quickly deplete the population of excitons, resulting in the PL intensity reduction. The annihilation of the excitons is reduced when a small number of excitons are excited (lower laser power regime).

Although PL is stable for fixed suspended segments, small variations of the emission wavelength as well as the FWHM of the spectra line were observed from different suspended segments under various laser power as shown in Fig. 4. For

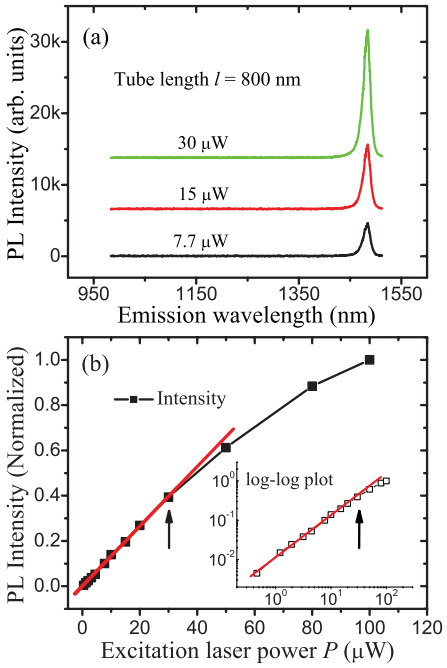

FIG. 3. (Color online) (a) Nanotube emission spectra at excitation powers of 7.7 (black), 15 (red), and 30 μW (green) for tube length $l = 800$ nm. The spectra are shifted for clarity. (b) Excitation laser power dependence of photoluminescence intensity. Inset shows a log-log plot. The linear fittings at lower power regime are shown by the solid red lines. Black arrows indicate the onset laser power (30 μW) for nonlinearity.

instance, at $P = 30$ μW, the measured standard deviations of the emission wavelength and spectral FWHM from $l = 200$ to 800 nm are 4.2 and 0.5 nm, respectively. The variations of the emission wavelength with tube length may be attributed to the strain imposed from the unsuspended segments, because the nanotubes are distorted by the interaction with the substrate surface.[18] Strain can be created on the suspended segments, which can cause mollification of the electronic band structure,[19] and a large effect is expected for a short suspended segment.

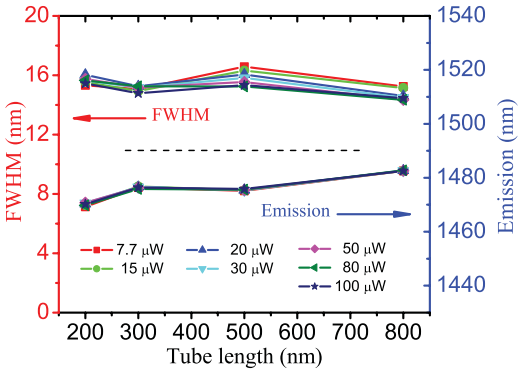

FIG. 4. (Color online) Emission wavelength (bottom) and FWHM (upper) of photoluminescence emission peak as a function of tube length under different excitation laser powers.

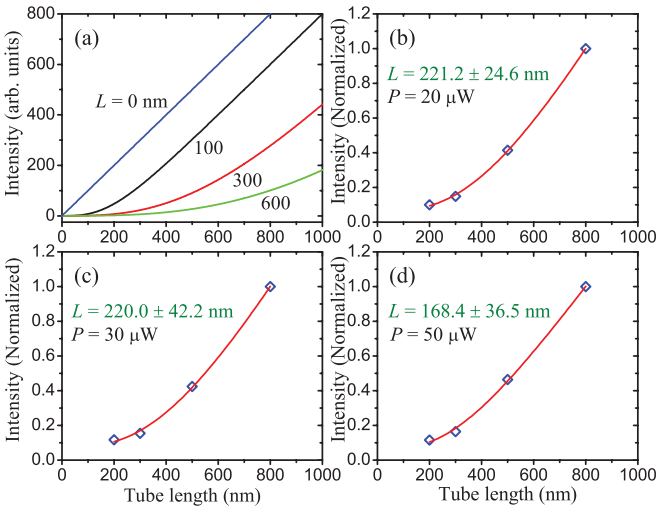

FIG. 5. (Color online) (a) Simulated PL intensity as a function of tube length for diffusion length $L = 0$ (blue), 100 (black), 300 (red), and 600 nm (green), respectively. (b)–(d) show the measured PL intensity as a function of tube length for laser power $P = 20$, 30, and 50 μW, respectively. The solid red lines represent the data fittings (see text).

B. Analysis of exciton diffusion length

PL originates from the recombination of excitons; hence, the PL intensity is determined by the total number of bright excitons in SWNTs. Due to the diffusive nature, excitons can diffuse a significant path before they recombine. The exciton density $n(z)$ which determines the PL intensity varies along the suspended SWNT segments. $n(z)$ is expected to decrease from the groove center to both edges (quench sites). The exciton dynamics in SWNTs can be described by the 1D diffusion equation.[6,7] In order to obtain the intrinsic diffusion length from the dependence of the PL intensity on nanotube length l, we first simulated the exciton density profile based on a steady-state 1D diffusion equation which is given by

$$D\frac{d^2n(z)}{dz^2} - \frac{n(z)}{\tau} + \Gamma(z) = 0. \quad (1)$$

The first term accounts for the exciton diffusion; the second term describes the radiative decay process; and the last term $\Gamma(z)$ is the exciton generation rate. Since our laser spot size is larger than the suspended segments studied here, which represents a broader laser beam intensity profile, we here assume that the exciton along the z is homogeneously generated resulting in a constant generation rate $\Gamma(z) = \Gamma$. Based on the boundary condition, $n(\pm l/2) = 0$, Eq. (1) can be solved to $n(z) = \Gamma\tau[1 - \cosh(z/L)\cosh^{-1}(l/2L)]$. Consequently, the entire PL intensity I from a certain segment can be obtained by integrating the exciton density profile,

$$I = \int_{-l/2}^{+l/2} n(z)dz = \Gamma\tau[l - 2L\tanh(l/2L)]. \quad (2)$$

The simulated PL intensity for a range of nanotube lengths and a series of diffusion lengths are plotted in Fig. 5(a). The PL intensity goes up quickly with l for shorter L. PL intensity scales linearly with tube length when L equals zero as shown by the blue line in Fig. 5(a). On the other hand,

for a fixed l, larger L results in a relatively lower PL intensity, which indicates an inefficient recombination of exciton caused by diffusion process. As the L gets longer, excitons more easily diffuse to the edges (unsuspended segments) leading to significant substrate-induced nonradiative decay.

The experimental data for l dependence of PL intensity was fitted by Eq. (2) under each excitation laser power to extract L. All of the intensity from the spectra are read by the area under a Lorentzian fitting curve. For a fixed excitation laser power, the value of $\Gamma\tau$ is counted as a constant; hence, the PL intensity is only a function of tube length and diffusion length. Figures 5(b)–5(d) show the measured PL intensity as a function of tube length at $P = 20$, 30, and 50 μW, respectively. The solid lines represent the best fits, which give $L = 221$, 220, and 168 nm for Figs. 5(b)–5(d). The variability of data is estimated by the error bar in all graphs. The relative error was around 10–20 %. Equation (1) is a simple steady-state diffusion model, which considers an effective 1D constant diffusion coefficient. The PL intensities were obtained from emission spectra which were collected for 180 s under a high signal to noise ratio, and we assumed a constant background signal in the experiment. During data fitting, a parameter was inserted in Eq. (2) to describe the background signal. A constant offset of the fitting lines is found, which is probably attributed to the constant background signal of the PL measurement system.

The diffusion length is plotted as a function of laser power in Fig. 6(a). For the lower laser power, $P \leqslant 30$ μW, the diffusion length scatters from 188 to 237 nm. However there is no obvious laser power dependence, and the average value is 219 nm as shown by the solid red line in Fig. 6(a). The lower laser power corresponds to a lower exciton density where the EEA is negligible. Hence, the diffusion length in the lower power regime is expected to be the intrinsic diffusion length of excitons in SWNTs, which means excitons can diffuse a significant distance within their intrinsic lifetime before their recombination. The exciton diffusion lengths previously reported in the surfactant- or DNA-wrapped SWNT samples are shorter than those evaluated in our long suspended SWNT.[3–6] This is probably due to the environment-induced exciton scattering or defect-related exciton trapping states in those samples.[20] Similar L values have been reported for other air-suspended SWNTs, about $\sqrt{2}L = 200$ nm by PL imaging[8] and $L = 280$–610 nm by length dependent PL from different tubes.[7] For the latter,[7] although the EEA was not taken into account, the results showed an obvious laser power dependence due to the EEA effect. On the other hand, the existence of tube to tube variations can also reduce the reliability of the data.

C. Analysis of laser power dependence

For $P > 30$ μW, the power-dependent decay behavior of L has been observed as presented in Fig. 6(a) in the large power regime. One can conclude that the onset power is consistent with that of EEA in SWNT. Excitons can be rather efficiently eliminated at high densities through the EEA process which is in agreement with previous claims.[15,21] This would explain the decay of PL intensity and exciton diffusion length with increasing laser power as shown in Fig. 3(b) and Fig. 6(a), respectively. The lifetimes of excitons

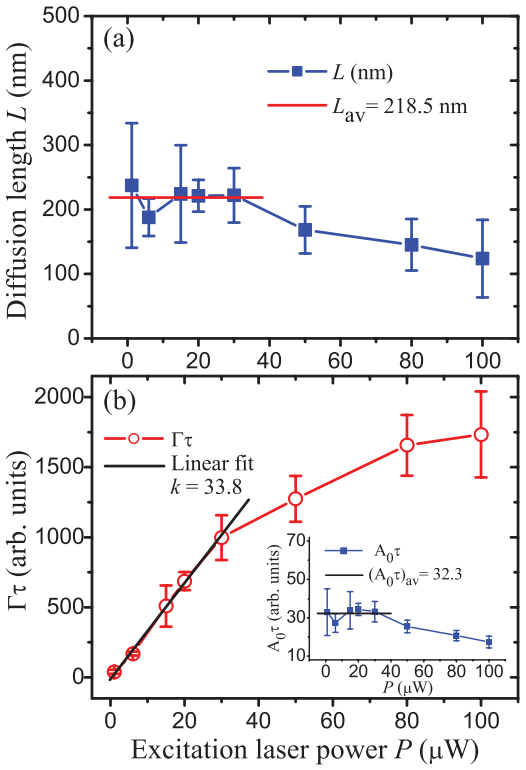

FIG. 6. (Color online) (a) Excitation laser power dependence of exciton diffusion length. The solid red line indicates the average value of diffusion length in the low-power regime. The reduction of the diffusion length in the high-laser-power regime is due to the EEA effect. (b) $\Gamma\tau$ as a function of laser power. The solid black line shows the linear fitting in the low-power regime. $A_0\tau$ as a function of laser power is shown in the inset. The solid black line gives the average value of $A_0\tau$ in the low-power regime.

are regarded to be reduced due to EEA.[3] For a higher laser power, the excitons only diffuse a mean-free path before the annihilation or recombination occurs due to EEA, and finally, the mean-free path is expected to be determined by a maximum density.

In the main graph of Fig. 6(b), we plotted $\Gamma\tau$ as a function of laser power after data fitting. $\Gamma\tau$ is found to be proportional to P at the lower power regime, while for P larger than 30 μW, $\Gamma\tau$ begins to deviate from the linear behavior. The onset laser power is consistent with those in the PL intensity and diffusion length cases shown in Fig. 3(b) and Fig. 6(a).

We assume that, for the first-order approximation, at the lower laser power regime with a lower exciton density where EEA effect is negligible, τ is constant indicating an intrinsic lifetime of excitons, and also Γ is proportional to P, i.e., $\Gamma = A_0 P$ with A_0 as the proportional constant. Consequently, $\Gamma\tau$ scales linearly with P, $\Gamma\tau = A_0\tau P$, as shown in the main graph of Fig. 6(b) (linear part). The value of $A_0\tau$ relating to the exciton lifetime is given by the slope k from the linear fitting [solid black line with $k = 33.8$]. On the other hand, $A_0\tau$ as a function of P shown by the inset can be deduced from the main graph of Fig. 6(b), i.e., $A_0\tau = \Gamma\tau/P$. The scaling behavior of $A_0\tau$ is analogous to the diffusion-length case. For $P \leqslant 30$ μW, the $A_0\tau$ is approximately a constant value (32.3 on average) presented by solid black line in the

inset. For higher P, $A_0\tau$ decaying quickly with laser power again provides evidence for the onset of the EEA effect in SWNTs. The reduction of the exciton lifetime in the high power regime may be responsible for the decrease of diffusion length [see Fig. 6(a) and the inset of Fig. 6(b)]. The laser power independence for both L and τ in the lower power regime allow us to conclude that exciton shows an intrinsic diffusion behavior. L and τ can be regarded as the intrinsic diffusion length and lifetime in this regime, respectively.

Analysis of the PL spectra intensity, exciton diffusion length, and lifetime depending on laser power enables us to identify that the lower threshold laser power, about 10^{21} photons/(cm^2 s), is consistent with the onset of EEA for air-suspended SWNTs. Most previous works reported the onset of sublinearity at much higher excited laser power (several orders of magnitude).[15,16,20] Moreover, there exists an upper limit to the exciton density in SWNTs caused by the EEA.[15,16] The laser power for the PL saturation (data not shown here) observed for our suspended SWNT sample is about 1.0 mW corresponding to an excitation photon fluence of about 10^{23} photons/(cm^2 s) which is much lower than the values reported by Högele *et al.*[22] and Murakami *et al.*[15] for encapsulated SWNTs with a pump fluence of about 10^{26} photons/(cm^2 s) and one order of magnitude lower than that measured by Xiao *et al.* for air-suspended SWNTs with a pump fluence of about 10^{24} photons/(cm^2 s).[16] The longer diffusion length and lifetime in an air-suspended SWNT may account for the lower EEA threshold, because the EEA threshold is inversely proportional to L and τ. Under $P = 30$ μW, the exciton density, with τ on the order of 10^2 ps,[16,23] is estimated to be about 1 in a 200-nm-long segment, if we assume that the quantum efficiency is about 7%.[24] The onset of EEA occurring at a low exciton density calls for new consideration of the nature of exciton interactions in a quasi-1D system.[16]

The particularly useful feature of excitons is that they can be generated by and converted back into a photon, opening the door for all sorts of ultrasmall optical switches and modulators.[25] The observed long intrinsic diffusion length in SWNTs at room temperature is much significant and is believed to pave the way for the development of new optoelectronic devices. The intrinsic diffusion length can give us some insight into the diffusion coefficient for excitons in SWNTs. Based on the reported exciton lifetime where τ is about 85 ps,[16] from $L = 200$ nm, one can obtain the diffusion coefficient $D = L^2/\tau \sim 5$ cm^2 s^{-1}, which is 3–4 orders of magnitude higher than those in organic semiconductors[26,27] and one order of magnitude larger than that in surfactant-wrapped SWNT samples,[3,4] although the accuracy of exciton lifetime should be considered in general.

IV. CONCLUSIONS

We developed a SWNT-sample structure for evaluating the intrinsic diffusion length of excitons in an individually suspended long SWNT by photoluminescence spectra. A freely suspended SWNT is an ideal sample to study fine structures and intrinsic optical properties of excitons. The results showed that the intrinsic diffusion length of excitons in SWNTs was as large as 200 nm. We discussed the process of exciton-exciton annihilation as a possible mechanism to explain the reduction of diffusion length with increasing excitation laser power. An onset laser power to nonlinearity of PL intensity consistent with EEA was found of about 10^{21} photons/(cm^2 s) for our air-suspended SWNT. Further precise works on the exciton diffusion length evaluation from suspended SWNTs should be performed on the same or several chiralities in vacuum or other environments.

ACKNOWLEDGMENTS

The work was supported partially by a Grant-in-Aid for Scientific Research on Priority Area (No. 19054015) from the Ministry of Education, Culture, Sports, Science, and Technology (MEXT) of Japan and CREST in the Japan Science and Technology Agency.

*jpxie@rs.kagu.tus.ac.jp
†homma@rs.tus.ac.jp

[1] T. Ando, J. Phys. Soc. Jpn. **66**, 1066 (1997).
[2] F. Wang, G. Dukovic, L. E. Brus, and T. F. Heinz, Science **308**, 838 (2005).
[3] L. Cognet, D. A. Tsyboulshi, J.-D. R. Rocha, C. D. Doyle, J. M. Tour, and R. B. Weisaman, Science **316**, 1465 (2007).
[4] L. Lüer, S. Hoseinkhani, D. Polli, J. Crochet, T. Hertel, and G. Lanzani, Nature Phys. **5**, 54 (2009).
[5] C. Geotgi, M. Böhmler, H. Qian, L. Novotny, and A. Harschuh, Phys. Status Solidi B **246**, 2683 (2009).
[6] A. J. Siitonen, D. A. Tsyboulski, S. M. Bachilo, and R. B. Weisman, Nano Lett. **10**, 1595 (2010).
[7] S. Moritsubo, T. Shimada, Y. Murakami, S. Chiashi, S. Maruyama, and Y. K. Kato, Phys. Rev. Lett. **104**, 247402 (2010).
[8] K. Yoshikawa, K. Matsuda, and Y. Kanemitsu, J. Phys. Chem. C **114**, 4353 (2010).
[9] H. Liu, D. Takagi, S. Chiashi, and Y. Homma, Nanotechnology **20**, 345604 (2009).
[10] Y. Homma, S. Suzuki, Y. Kobayashi, M. Nagase, and D. Takagi, Appl. Phys. Lett. **84**, 1750 (2004).
[11] J. Lefebvre, Y. Homma, and P. Finnie, Phys. Rev. Lett. **90**, 217401 (2003).
[12] S. M. Bachilo, M. S. Strano, C. Kittrell, R. H. Hauge, R. E. Smalley, and R. B. Weisman, Science **298**, 2361 (2002).
[13] R. B. Weisman and S. M. Bachilo, Nano Lett. **3**, 1235 (2003).
[14] S. Chiashi, S. Watanabe, T. Hanashima, and Y. Homma, Nano Lett. **8**, 3097 (2008).
[15] Y. Murakami and J. Kono, Phys. Rev. Lett. **102**, 037401 (2009).
[16] Y.-F. Xiao, T. Q. Nhan, M. W. B. Wilson, and J. M. Fraser, Phys. Rev. Lett. **104**, 017401 (2010).
[17] K. Matsuda, T. Inoue, Y. Murakami, S. Maruyama, and Y. Kanemitsu, Phys. Rev. B **77**, 033406 (2008).
[18] T. Hertel, R. E. Walkup, and P. Avouris, Phys. Rev. B **58**, 13870 (1998).
[19] L. Yang and J. Han, Phys. Rev. Lett. **85**, 154 (2000).

[20] A. Hagen, M. Steiner, M. B. Raschke, C. Lienau, T. Hertel, H. Qian, A. J. Meixner, and A. Hartschuh, Phys. Rev. Lett. **95**, 197401 (2005).
[21] Y.-Z. Ma, L. Valkunas, S. L. Dexheimer, S. M. Bachilo, and G. R. Fleming, Phys. Rev. Lett. **94**, 157402 (2005).
[22] A. Högele, C. Galland, M. Winger, and A. Imamoğlu, Phys. Rev. Lett. **100**, 217401 (2008).
[23] Y. Ohno, S. Iwasaki, Y. Murakami, S. Kishimoto, S. Maruyama, and T. Mizutani, Phys. Status Solidi B **244**, 4002 (2007).
[24] J. Lefebvre, D. G. Austing, J. Bond, and P. Finnie, Nano Lett. **6**, 1603 (2006).
[25] G. Grosso, J. Graves, A. T. Hammack, A. A. High, L. V. Butov, M. Hanson, and A. C. Gossard, Nature Photonics **3**, 577 (2009).
[26] A. J. Lewis, A. Ruseckas, O. P. M. Gaudin, G. Webster, P. L. Burn, and I. D. W. Samuel, Org. Electron. **7**, 452 (2006).
[27] O. V. Mikhnenko, F. Cordella, A. B. Sieval, J. C. Hummelen, P. W. M. Blom, and M. A. Loi, J. Phys. Chem. B **112**, 11601 (2008).